

PAPER

## Asymmetric toroidal eddy currents (ATEC) to explain sideways forces at JET

To cite this article: R. Roccella *et al* 2016 *Nucl. Fusion* **56** 106010

View the [article online](#) for updates and enhancements.

### Related content

- [Plasma current asymmetries during disruptions in JET](#)  
S.N. Gerasimov, T.C. Hender, J. Morris *et al.*
- [Measurement of scrape-off-layer current dynamics during MHD activity and disruptions in HBT-EP](#)  
J.P. Levesque, J.W. Brooks, M.C. Ablter *et al.*
- [JET and COMPASS asymmetrical disruptions](#)  
S.N. Gerasimov, P. Abreu, M. Baruzzo *et al.*

### Recent citations

- [Disruptive plasma simulations in EAST including 3D effects](#)  
S.L. Chen *et al*
- [Damping effect on the ITER vacuum vessel displacements during slow downward locked and rotating asymmetric vertical displacement events](#)  
Pietro Testoni *et al*
- [Reduction of asymmetric wall force in ITER disruptions with fast current quench](#)  
H. Strauss



**IOP | ebooks™**

Bringing you innovative digital publishing with leading voices to create your essential collection of books in STEM research.

Start exploring the collection - download the first chapter of every title for free.

# Asymmetric toroidal eddy currents (ATEC) to explain sideways forces at JET

R. Roccella<sup>1</sup>, M. Roccella<sup>2</sup>, V. Riccardo<sup>3</sup>, S. Chiochio<sup>1</sup>  
and JET Contributors<sup>a</sup>

EUROfusion Consortium, JET, Culham Science Centre, Abingdon, OX14 3DB, UK

<sup>1</sup> ITER Organization, Route de Vinon-sur-Verdon, CS 90 046, 13067 St Paul Lez Durance Cedex, France

<sup>2</sup> LTCalcoli Srl, Piazza Prinetti 26/B, 23807, Merate (LC), Italy

<sup>3</sup> CCFE, Culham Science Centre, OX14 3DB, Abingdon, UK

E-mail: [riccardo.roccella@iter.org](mailto:riccardo.roccella@iter.org)

Received 13 October 2015, revised 4 March 2016

Accepted for publication 30 March 2016

Published 9 August 2016



CrossMark

## Abstract

During some JET vertical displacement events (VDEs) plasma current and position are found to be toroidally asymmetric. When asymmetries lock, the vessel has been observed to move horizontally, consequently strong horizontal forces are expected following plasma asymmetries, whether locked or rotating. The cause of horizontal forces is, as already identified in previous works, the asymmetric circulation of current in the structures. The physics mechanism responsible for these asymmetric currents is instead an open issue and it is the object of the present analysis. In particular it will be shown that the asymmetry is not due to a direct exchange of current between plasma and structure (as in the case of halo currents) but to asymmetric conductive paths which arise, in the structures, when the plasma column asymmetrically wets the wall. Simulations of this phenomenon using finite element (FE) models have been conducted to reproduce the JET observation during locked and rotating asymmetric VDEs. Estimated sideways force, asymmetry ( $I_p^{\text{asym}}$ ) and normalized asymmetry ( $A_p^{\text{asym}}$ ) of plasma current, vertical position at different toroidal locations during the disruption and halo current asymmetry have been compared with measurements done at JET during upward AVDEs. The substantial match between experiments and simulations confirms the soundness of the assumptions. Furthermore, the same physical model applied to downward VDEs shows that divertor support and coils, together with the geometry of the limiting surfaces, considerably lessen asymmetric loads as experienced at JET after installing those components.

Keywords: JET, ITER, asymmetric vertical displacement events, sideways forces, halo currents, ATEC

(Some figures may appear in colour only in the online journal)

## 1. Introduction

Plasma asymmetries during VDEs are measured in several tokamaks (JET [1], ASDEX upgrade [2], DIII-D [3]) but evidence of associated strong asymmetric loads are observed only at JET.

These observations provide, in ITER, the basis for definition of asymmetric VDE loads. They are assessed, using the

source and sink model, through extrapolation of the amplitude of the plasma current asymmetry and duration from JET. The source and sink model gives a quantitative estimate of the sideways force consistent with the measured JET vessel displacement. Applied to ITER vacuum vessel (VV) analyses the same model predicts about 45 MN of sideways forces in locked AVDEs [4]. In case of asymmetry rotating at frequencies close to the ITER VV natural frequency the VDE duration extrapolated from JET data, would cause important amplification of the vessel deformations. In addition to these loads,

<sup>a</sup> See the appendix of [9].

the halo current asymmetry measured during AVDEs would produce relevant tilting moments on the ITER structures. Understanding the causes of sideways forces and of asymmetric halo currents measured in JET during AVDEs is, then, essential to confirm the basis for the loads estimate on the ITER VV and it is the aim of this analysis.

In the following sections, we present a model for locked and rotating Asymmetric VDEs (AVDEs) which:

- provides a likely explanation of the phenomenon of the AVDEs showing the mechanism triggering the asymmetric flow of current in the structures;
- is consistent with the JET magnetic measurements during upward AVDEs;
- is consistent with the sideways forces predicted by the source and sink model and inferred from JET vessel displacement during AVDEs;
- demonstrates the fundamental identity between measured plasma and halo current asymmetries;
- explains why, at JET, the divertor structure prevents the raise of asymmetric loads during downward VDEs.

## 2. AVDE sideways force mechanism

The JET disruption shown in figure 1 (38070, [1]) caused large sideways displacement and is a clear case of locked AVDE. The minimum and maximum asymmetry of toroidal plasma current ( $I_p$ ) and vertical position ( $z_p$ ) are measured at octant 3 and 7 respectively and do not move significantly during the disruption.

During the current quench the asymmetric instability arises and pushes one side (octant 7) of the plasma column against the in-vessel upper structures that at the date of this event were Inconel dump plates (DP) covered with carbon fibre composite (CFC) tiles. At the opposite side of the torus, octant 3, no significant vertical movement is measured. The asymmetry starts with the plasma column already displaced 1.25 m upward and the average difference in vertical position during the current quench (CQ) phase is about 0.2 m. During the asymmetric phase the first wall (FW) surface at the top of the machine deeply intersects the plasma column around octant 7. Under certain conditions of plasma temperature (and thus resistivity) it is possible that neighbouring dump plates are short-circuited in toroidal direction through the plasma. In this configuration, part of the toroidal current induced in the vacuum vessel (VV), which has the same sign as the plasma current, will flow in the dump plates of the sectors wetted by the plasma. On the opposite side of the machine (around octant 3), where the plasma and structure are not in contact the short circuit cannot be established. A schematic view of the asymmetric path of the induced current is shown in figure 2(a). The eddy current (green) is induced only in the vacuum vessel where the plasma vertical position is measured low (octant 3) but where the plasma wets the structure, part of it is transferred to the dump plates. The poloidal path of the eddy current from the VV to the DPs in octants 3 to 7 (and its anti-symmetric counterpart from the DPs to the VV on the opposite side of the machine) interacts with the toroidal field resulting in a net sideways force. Figure 2(lower part) shows a simplified view of the kink mode configuration of

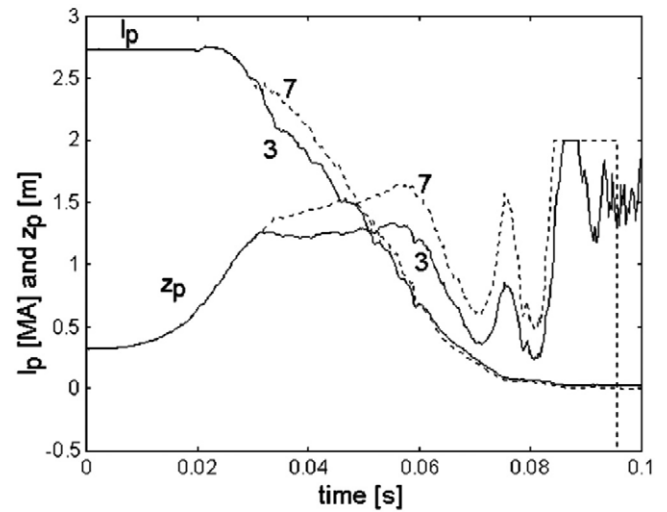


**Figure 1.** JET AVDE (pulse 38070) with measured plasma current and vertical position in two opposite octants. Reproduced with permission from [1], copyright 2000 IOP Publishing Ltd.

pulse 38070. In the octant 3 the entire induced toroidal current flows in the vessel and only the plasma current is measured by the pick-up coils; in the octant 7 the part of induced current that flows toroidally in the dump plates falls inside the contour of in-vessel poloidal field pick-up coils (in red) and contributes to the measure of the plasma current.

This scheme implies that the plasma current is the same at all toroidal locations. The measured asymmetry is not due to plasma current which, in some sectors, flows toroidally in the vessel as it would be in case of toroidal halo current. The cause of the asymmetry is, instead, current induced in the vessel structures which flows internally to the pick-up coils loop where the plasma column wets the top dump plates.

## 3. Analysis models

Two finite element models have been prepared in ANSYS® to assess locked (180° model) and rotating (360° model) AVDEs.

The geometry is based on JET CAD drawings of the vacuum vessel and includes sector double shell, port openings and bellows.

All modelled structures except for the CFC tiles and, of course, the halo current (HC) region, are made of Inconel. The assigned resistivity is:  $1.3 \cdot 10^{-6} \Omega\cdot\text{m}$  for vessel bosses and dump plates and  $5 \cdot 10^{-6} \Omega\cdot\text{m}$  for CFC tiles. The bellows are simulated with straight plates of 3 mm thickness with an orthotropic equivalent resistivity calculated of  $1.4 \cdot 10^{-6} \Omega\cdot\text{m}$  radially and poloidally resistivity and  $5 \cdot 10^{-6} \Omega\cdot\text{m}$  toroidally. The resulting toroidal resistance of JET vessel is  $R_{\text{tor}} \sim 370 \cdot 10^{-6} \Omega$  against an expected value of about  $330 \cdot 10^{-6} \Omega$  reported in [5].

## 4. Procedure for calculation of locked and rotating AVDE

The plasma AVDE is described via finite element (FE) models as following: the plasma current is approximated by means of

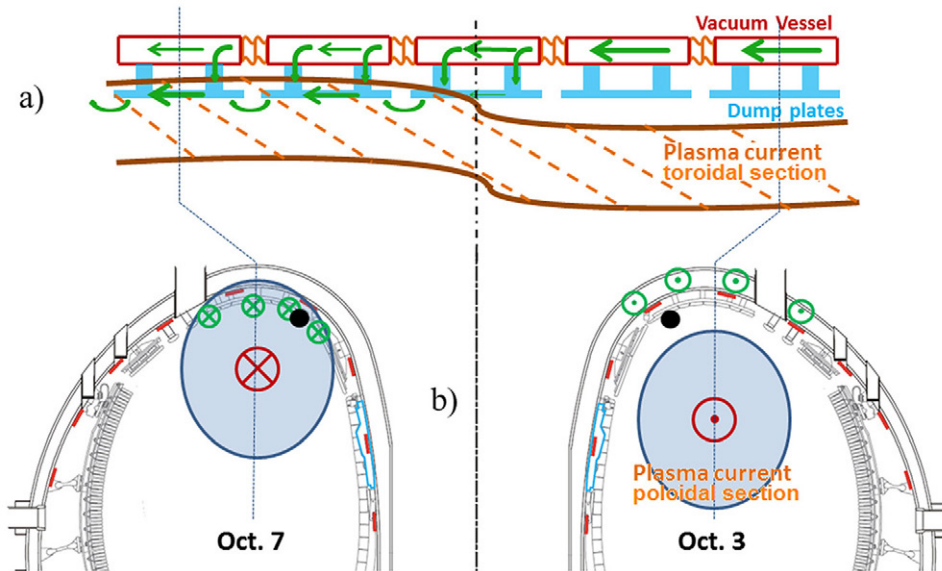


**Figure 2.** Schematic view of eddy current patterns in JET structures during AVDEs. Toroidal section at vessel top (a); vertical section of the machine (b). The black spots approximately indicate the location of the toroidal field pick-up coils.

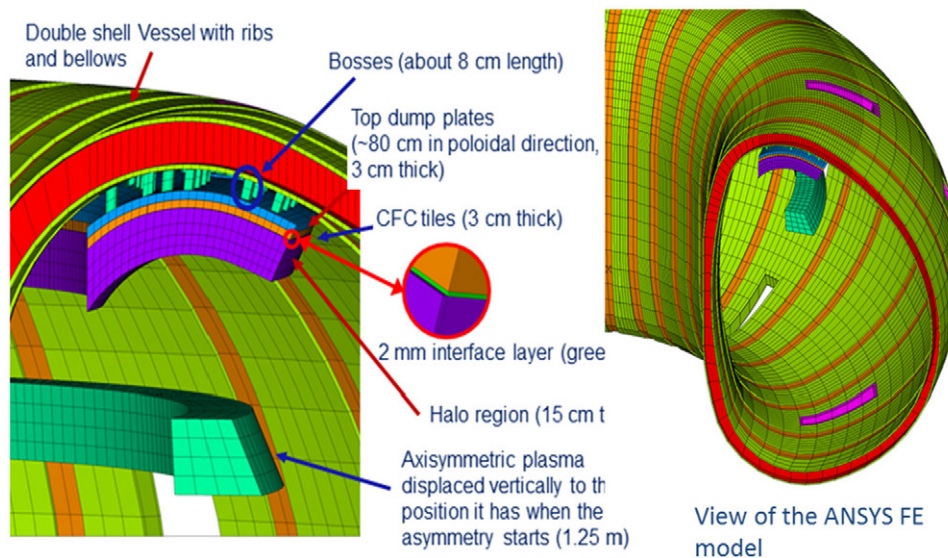


**Figure 3.** Detail of the upper region: an axisymmetric 15 cm halo region (purple) wets the CFC tiles (orange elements). The resistivity of the contact element (green) between halo region and CFC tiles changes with the toroidal angle (with the function of figure 4). The plasma current, located in the vertical position it has when the asymmetry starts is also axisymmetric.

a set of axisymmetric elements (green in figure 3) located at the vertical position of the plasma when the asymmetry starts,  $z_p = 1.25$  m (from figure 1). The plasma elements are not conductive (in this way no eddy current is induced in these elements during transients) and a total current ( $I_p$ ) is imposed to reproduce the current quench behaviour from 2.7 MA linearly down to 0 in about 40 ms.

A halo region (HR) of about 15 cm radial width is in contact with the dump plates through a thin (2 mm) interface layer. The halo region is, like the plasma, an axisymmetric component and covers most part of the dump plates in the poloidal direction. The halo region resistivity is evaluated through Spitzer's formula [6]:  $\eta_{\parallel} = 2.8 \cdot 10^{-8} / T_e^{3/2}$  ( $\Omega \cdot m$ ) with  $T_e$  in keV for the component of current parallel to the

magnetic field and  $\eta_{\perp} = 1.96 \cdot \eta_{\parallel}$  for the component of current perpendicular to the magnetic field.

Several cases have been analysed for electron temperatures in the range between  $5 \cdot 10^{-3}$  and  $2 \cdot 10^{-2}$  keV which correspond to parallel resistivity between  $7 \cdot 10^{-5}$  and  $8 \cdot 10^{-6}$   $\Omega \cdot m$  and normal resistivity about two times higher. The resistivity of the HR is thus orthotropic. It has been assigned equal to the parallel resistivity in the toroidal and in the poloidal direction, and to the normal resistivity in the radial direction.

The asymmetry is reproduced by changing the radial resistivity of the thin interface layer between HR and CFC tiles with the toroidal angle. At low toroidal angles the resistivity is set very high preventing short-circuit of CFC tiles then it gradually decreases (in the toroidal direction) to simulate the

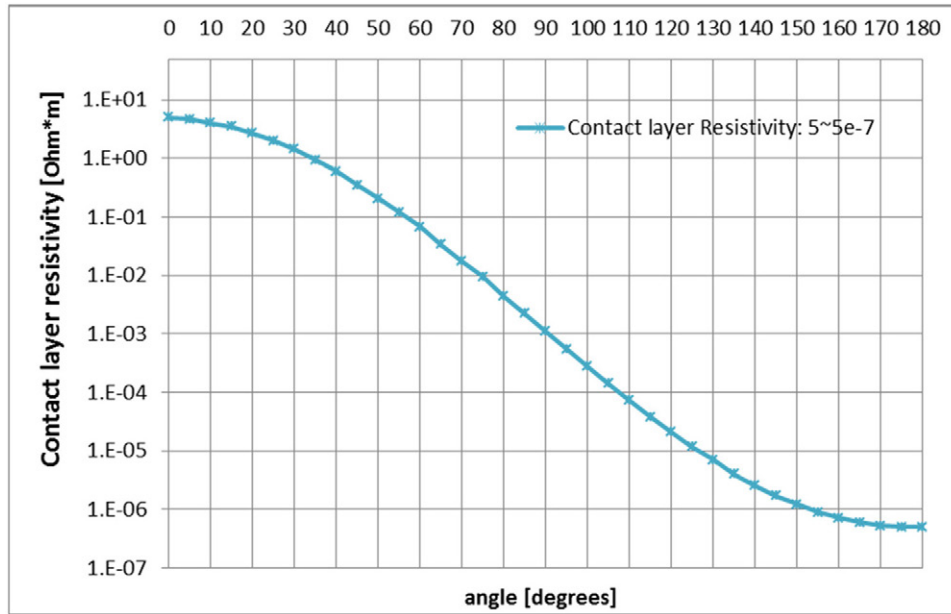


Figure 4. Resistivity of the thin interface layer between plasma HR and CFC tiles.

increase of wetting area associated with the asymmetry evolution. The curve of resistivity versus toroidal angle is shown in figure 4. Variation in the curve would impact the distribution of the asymmetry in the toroidal direction.

The sideways force ( $F_y$ ) is evaluated by the following formula:

$$F_y = 2 \cdot \sum_1^{n_{el,180}} J_z(i) \cdot B_{tor}(i) \cdot vol(i) \quad (1)$$

Where  $n_{el,180}$  are all elements of conducting structures in the 180° model (vessel, bellows, dump plates and their connecting bosses and CFC tiles);  $J_z(i)$  is the vertical component of the current density in the generic element  $i$ ;  $vol(i)$  the volume of the element  $i$  and  $B_{tor}(i)$  is the toroidal field at the location of the element  $i$  consistent with the toroidal field of the analysed pulse of 2.85 T at 3 m from the tokamak axis. In the analysis of the rotating AVDE the same sum is extended to all elements of the 360° model and the resulting force is not doubled.

The net toroidal current in the HR is prevented (by isolating its nodes at the 0° boundary) to make sure that the overall current quench time is not modified by this current.

A similar procedure has been applied to a 360° FE model for the rotating case with the difference that after the first 10ms of locked asymmetry, it starts rotating and completes 5 revolutions in 30ms (during the last 10ms of the current quench no rotation is imposed). The plasma temperature for the rotating case has been assumed around 15 eV.

#### 4.1. Asymmetries during upward VDEs

Several cases have been analysed to verify whether the proposed model is able to reproduce the typical locked AVDE measurements of JET pulse 38070. Sideways force and asymmetry of the plasma current have been assessed for a range of plasma parallel resistivity which goes from  $10^{-5}$  to

$7 \cdot 10^{-5} \Omega \cdot m$  (roughly corresponding to temperature of pure hydrogen plasma from 20 to 5 eV). The amplitude ( $I_p^{asym}$ ) and the normalised amplitude ( $A_p^{asym}$ ) of the plasma current asymmetries [7] are calculated as:  $I_p^{asym} = \sqrt{(I_{p7} - I_{p3})^2}$  for locked AVDE analysis,  $I_p^{asym} = \sqrt{(I_{p7} - I_{p3})^2 + (I_{p5} - I_{p1})^2}$  for rotating AVDE and  $A_p^{asym} = I_p^{asym} / |I_p^{dis}|$  for both locked and rotating AVDE. Another relevant measured parameter is the first plasma current vertical (and radial) moment which gives the position of the plasma centroid normalized over the total current; it has been deduced as following from the simulation results:  $M_{Iz} = \sum_i J_i^{tor} \cdot A_i \cdot Z_i$  where  $J_i^{tor}$  is the toroidal component of current density in the element  $i$ ;  $A_i$  is the area of element  $i$  orthogonal to the toroidal direction and  $Z_i$  is the vertical position of the element  $i$ . The sum is extended to all elements carrying toroidal current inside the vacuum vessel. The plasma current (calculated at octants 1, 3, 5, and 7), plasma current asymmetry and calculated vertical position are shown in the following figure 5 and should be compared with the measurements of the target pulse 38070 (figure 1). In the simulations, the initial slow vertical drift of the plasma is not taken into account as it is located at the position occupied at the asymmetry onset.

In figure 5,  $I_{p\_oct3}$  indicate the total toroidal current inside the poloidal field pick-up coils loop at octant 3 (0°) and  $I_{p\_oct7}$  the current at octant 7 (180°) for plasma temperatures from 5 to 20 eV;  $DI_p$  is the plasma current asymmetry (total current at octant 7–octant 3);  $z_{p\_max}$  is the vertical position of plasma current centroid calculated at octant 7.

The asymmetry of the plasma current ( $I_p^{asym}$ ) is extracted from the simulation results approximately every 12° (at the VV bellow locations) and is shown, together with the current entering in the DP from the vessel at each assessed toroidal location, in figure 6. For the locked AVDE case it gives 10% of  $A_p^{asym}$ . The  $I_p^{asym}$  is evaluated by the line integral of  $B$  along

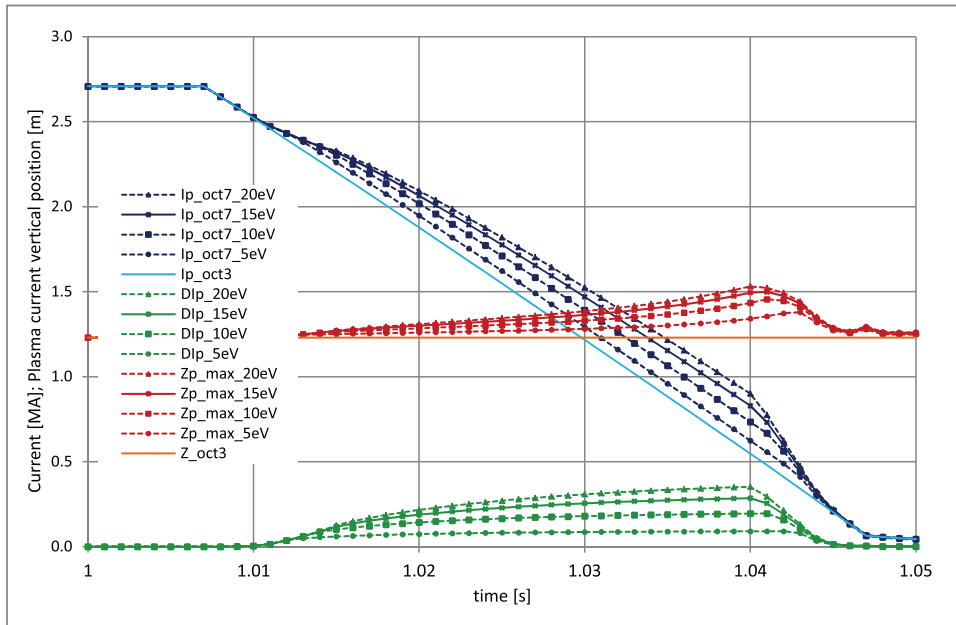


**Figure 5.** FE simulation results of JET pulse 38070 with plasma temperature between 5 and 20 eV: plasma current plasma (blue lines) and plasma centroid vertical positions (red lines) in two opposite octants (3 and 7); in green the plasma current asymmetry.

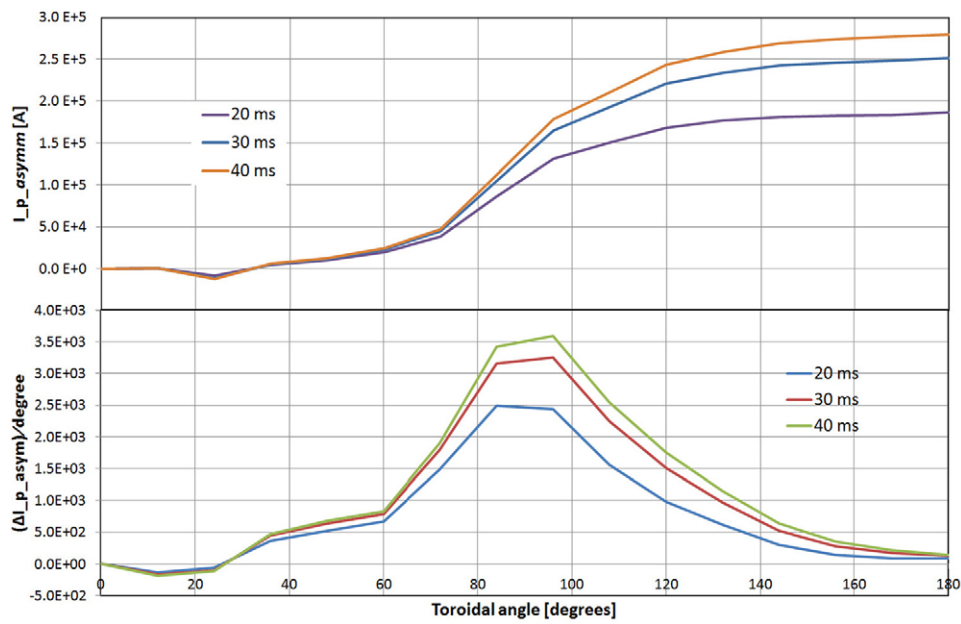


**Figure 6.** Toroidal current flowing in the dump plates versus the toroidal angle and angular current density flowing from VV to dump plates versus toroidal angle.

**Table 1.** Values of plasma temperature and resistivity and main locked AVDEs simulation results.

Plasma temp.	Parallel resistivity ( $\Omega \cdot m$ )	Normal resistivity ( $\Omega \cdot m$ )	Max plasma current asymmetry (kA)	Max normalized plasma current asymmetry	Max plasma vertical asymmetry (m)	Max sideways force (MN)
5 eV	$7.92 \cdot 10^{-5}$	$1.58 \cdot 10^{-4}$	91	0.033	0.15	0.85
10 eV	$2.8 \cdot 10^{-5}$	$5.6 \cdot 10^{-5}$	195	0.072	0.23	1.75
15 eV	$1.5 \cdot 10^{-5}$	$3 \cdot 10^{-5}$	285	0.105	0.27	2.5
20 eV	$1 \cdot 10^{-5}$	$2 \cdot 10^{-5}$	353	0.13	0.3	3.2

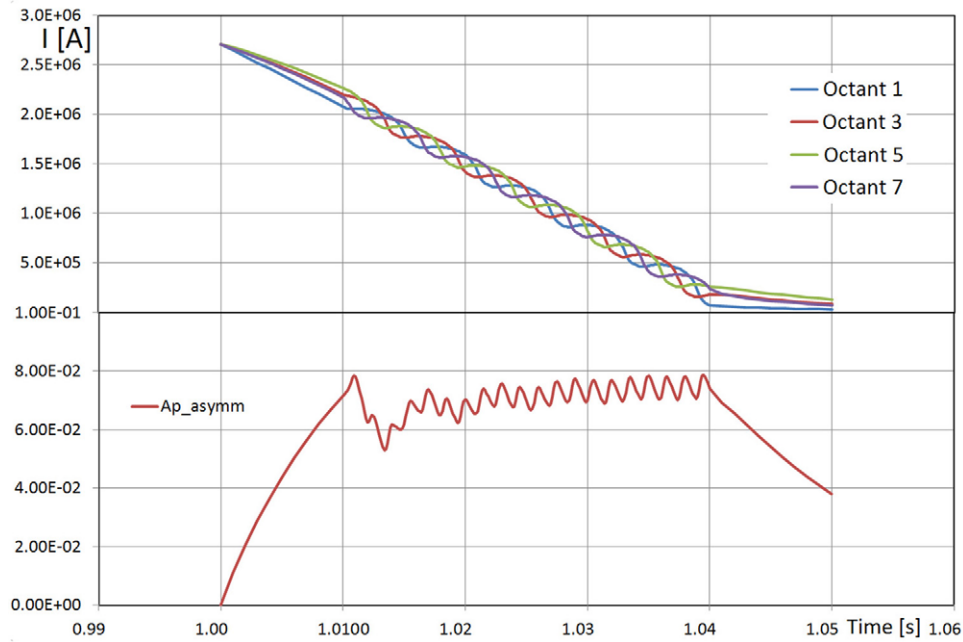


**Figure 7.** Top: calculated plasma current in 4 octants during a rotating AVDE (plasma temperature  $\sim 13$  eV); bottom: normalized amplitude of the plasma current asymmetry. The AVDE begins locked, at 10 ms the fast rotation starts completing 5 loops in 30 ms ( $\sim 170$  Hz).

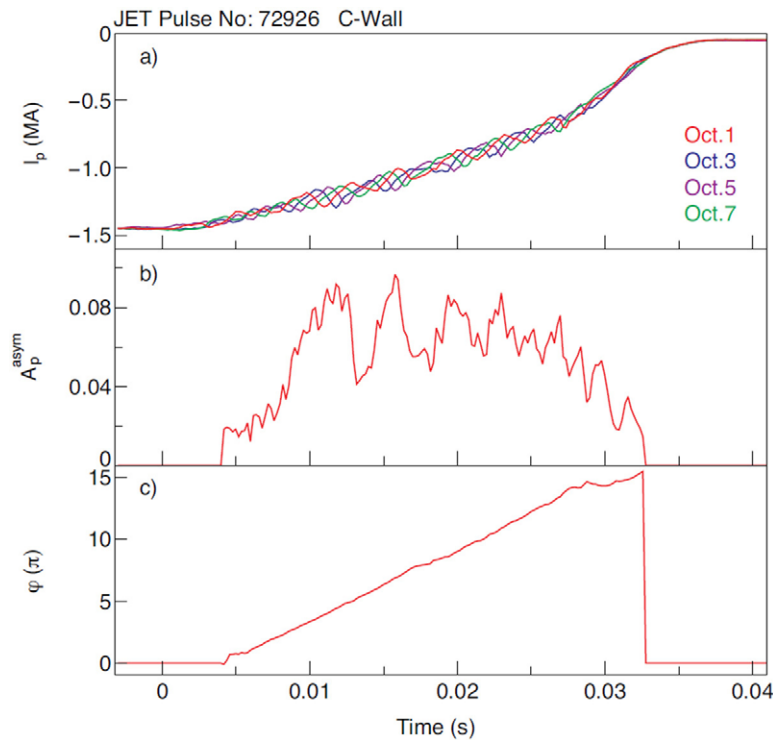


**Figure 8.** Measured plasma current in 4 octants, normalised asymmetry of plasma current and phase of the asymmetry rotation during JET pulse 72926. Reproduced with permission from [7], copyright 2014 EURATOM.

a path which follows the VV inner shell contour retracing the JET array of in-vessel poloidal pick-up coils (red dashes in figures 2 and 13). Table 1 summarises the imposed values for the plasma temperature and resistivity and the main simulation results ( $I_p^{\text{asym}}$ ;  $A_p^{\text{asym}}$ ;  $\Delta z_{\text{max}}$ ;  $F_y^{\text{max}}$ ).

So far, only one case of rotating AVDE has been analysed due to the demanding computational resources. The  $360^\circ$  FEM implements about 400 000 elements and the transient

simulation solved 260 time steps to reproduce the rotating event.

In order to assess the influence of the rotation on the sideways force the same case has been analysed with locked asymmetry.

The plasma current in the 4 octants (1, 3, 5 and 7) and normalised asymmetry are reported in figure 7 and should be compared with the JET measurements of pulse 72926 where

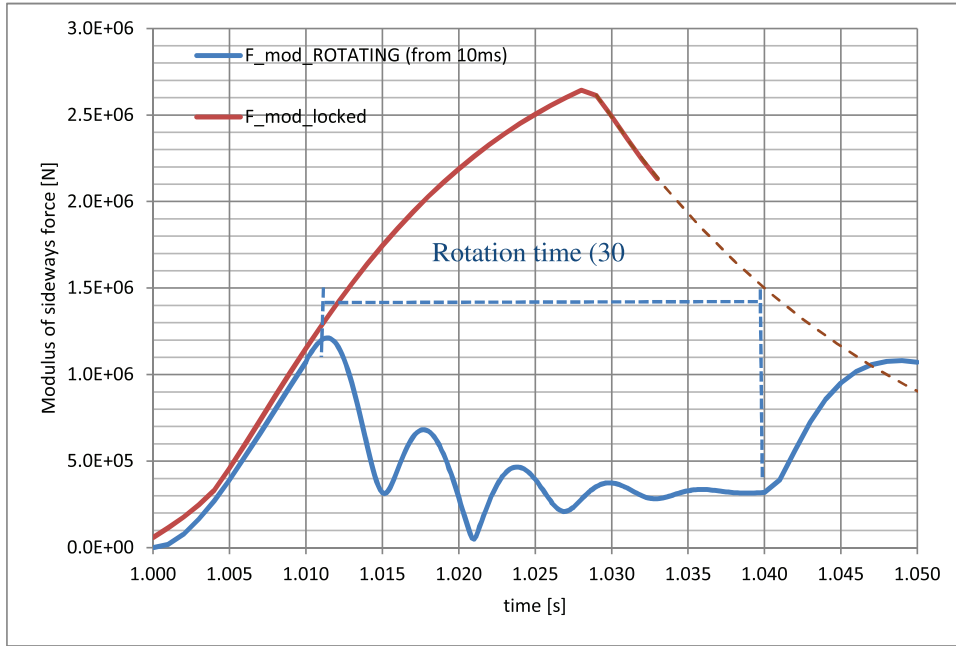


**Figure 9.** Comparison of calculated modulus of sideways force for locked and rotating AVDE (plasma current before disruption and current quench time are same for both cases).

5 rotations are completed in about 30 ms (figure 8 from [7]). Both the plasma current in the four octants and the normalised asymmetry are consistent with the simulation and a strong damping of the sideways force due to the rotation has been found. Figure 9 shows a reduction of almost one order of magnitude in the sideways force exerted during the rotating (blue) case with respect to the corresponding locked (red) case. It can be noticed that even though the  $A_p^{\text{asym}}$  is about 80% of the locked case (0.08 against 0.1 of the locked AVDE) the force that is produced by this asymmetry decreases to about 10% of the locked case.

The proposed model of ATEC implies that part of the difference in the plasma vertical position in opposite octants is not caused by the real plasma deformation ( $m = n = 1$  mode) but by the induced current flowing at a fixed height (dump plates). A clear phase relationship between the plasma current asymmetry ( $\Delta I_p$ ) and the first vertical current moment ( $\Delta M_{IZ}$ ) is thus expected as the latter is the sum of the moment of the current  $\Delta I_p$  flowing in the plates and the moment of quenching plasma current, which in the simulation does not change position (because the plasma kink is not modelled). The slope of the  $\Delta M_{IZ} - \Delta I_p$  phase relationship depends, then, in the FE analysis, only on the vertical position of the DP where the  $\Delta I_p$  flows:

$$\begin{aligned} \Delta M_{IZ}^{\text{FE}} &= M_{IZ}^{\pi} - M_{IZ}^0 = I_p \cdot z_p + \Delta I_p \cdot z_{\text{DP}} - I_p \cdot z_p \\ &= \Delta I_p \cdot z_{\text{DP}} \rightarrow \frac{\Delta M_{IZ}^{\text{FE}}}{\Delta I_p} = z_{\text{DP}} \end{aligned} \quad (2)$$

In JET, on the other hand, the measurement of  $M_{IZ}$  includes the kink of the plasma column:

$$\begin{aligned} \Delta M_{IZ}^{\text{JET}} &= I_p \cdot \left( z_p + \frac{\Delta z_{\text{kink}}}{2} \right) + \Delta I_p \cdot z_{\text{DP}} - I_p \cdot \left( z_p - \frac{\Delta z_{\text{kink}}}{2} \right) \\ &= I_p \cdot \Delta z_{\text{kink}} + \Delta I_p \cdot z_{\text{DP}} = \Delta M_{IZ}^{\text{kink}} + \Delta M_{IZ}^{\text{FE}}; \end{aligned} \quad (3)$$

where  $z_{\text{DP}}$  is the average vertical position of the top dump plate;  $\Delta z_{\text{kink}}$  and  $\Delta M_{IZ}^{\text{kink}}$  are respectively, the variations of plasma vertical position and plasma current first moment due to the kink only; superscripts FE and JET label quantities evaluated in the FE analysis or measured during JET experiments.

In the end, the difference between the simulated and the measured  $\Delta M_{IZ}$  is the variation of plasma current first moment due to the kink alone. This result is independent from the amplitude of  $\Delta I_p$  and from the assumptions on the plasma position made in the simulation.

Figure 10(left) shows the measured  $\Delta M_{IZ} - \Delta I_p$  phase relation: the slope is almost constant for all the reported disruptions and close to the slope of the evaluated phase relation equal to  $z_{\text{DP}}$  (figure 10(right)). This confirms that  $\Delta I_p$  is actually flowing at the DP level.

The small distance between the two lines at equal  $\Delta I_p$  gives, as shown above,  $\Delta M_{IZ}^{\text{kink}} (= \Delta M_{IZ}^{\text{JET}} - \Delta M_{IZ}^{\text{FE}})$ . This is much smaller than the measured  $\Delta M_{IZ}$  and of the same order of the measured  $\Delta M_{IZ}$  (0.05 ÷ 0.1) as expected in case of asymmetries dominated by an  $m = n = 1$  mode [7].

#### 4.2. Asymmetries during downward VDEs

Both upward and downward asymmetric VDEs were experienced at JET before installing the divertor coils and structure. After this major upgrade no relevant asymmetries have been measured during downward VDEs. The divertor structures prevent somehow plasma toroidal current asymmetries. Preliminary analysis of downward AVDEs have been carried out on the base on the hypothesis that, in case of plasma asymmetries, ATEC could also flow in the lower structures of the JET vessel.

The main structures added with the divertor upgrade are the four active divertor coils (green in figure 11) and, starting

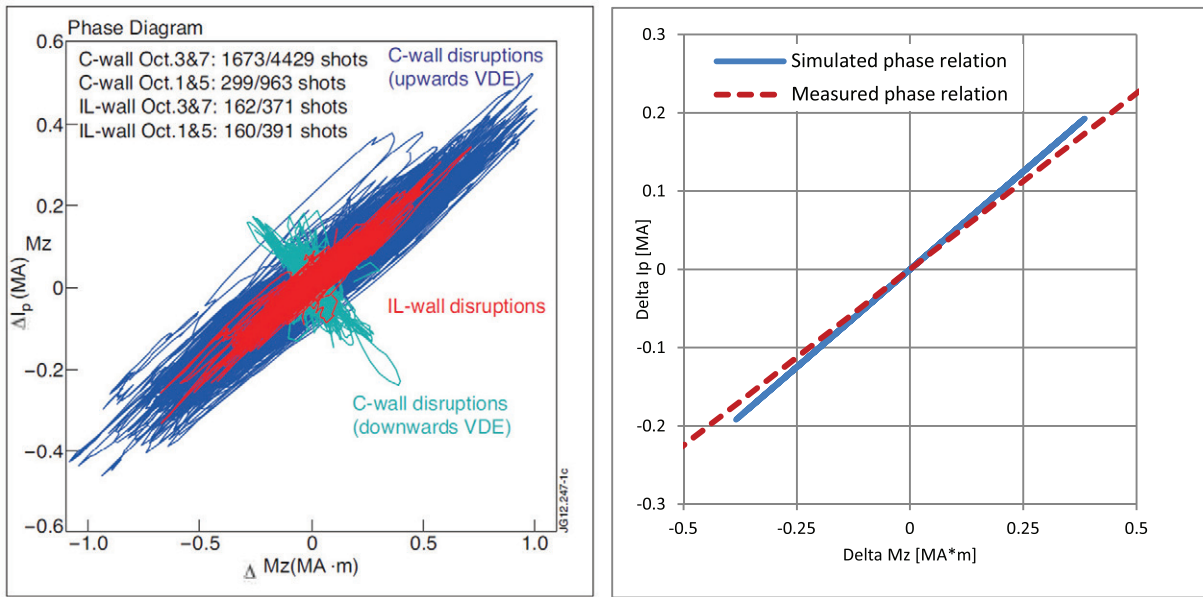


**Figure 10.** Measured (at JET left) and calculated (right) phase relationship between plasma current ( $\Delta I_p$ ) and first plasma current vertical moment ( $\Delta M_{Iz}$ ) asymmetries. Reproduced with permission from [7], 2014 EURATOM.

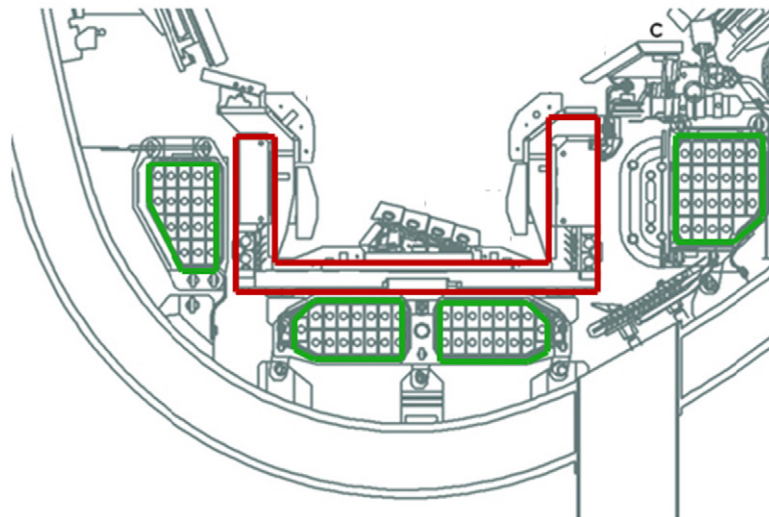


**Figure 11.** Toroidally continuous components in the divertor (MkII) region: divertor support structure (red) and divertor coils (green).

from MkII, the divertor support structure (red in figure 11). The coils (in copper) are made of 15–20 turns each (about 65 turns total). During disruptions they can be considered, in most cases, short-circuited through their power supplies. The divertor support is a toroidally continuous  $U$ -shaped Inconel structure of about 10 cm thickness. In case of downward VDEs important currents are induced both in divertor coils and support partly shielding the vessel for longer time than current quench duration.

In this qualitative analysis the AVDE of figure 1 has been simulated with the divertor structures modelled at the machine top, the halo temperature fixed to 15 eV and the plasma asymmetry modelled in the same way as in the upward AVDEs analyses. The divertor support has been modelled by connecting all top dump plates in toroidal direction and their resistivity has been modified to take into account that the divertor support is about three times thicker than the dump plates.

The divertor coils have been modelled by means of a single stranded coil, insulated from the rest of conductive structures, positioned between the dump plates and the vessel (orange elements in figure 12). The resistivity of the coil in the FE model has been chosen to allow comparable induced current to the total induced in the divertor coils during a downward VDE (about 15–20% of  $I_p$ ).

The analysis results show about one order of magnitude reduction in measured plasma current asymmetry ( $A_p^{\text{asym}} = 0.01$ ) and sideways force ( $F_y^{\text{max}} = 0.23$  MN) with respect to the corresponding upward case. Most part of the reduction is caused by divertor support. In fact the same analysis run without the divertor coil gives only slightly higher asymmetry and sideways force ( $A_p^{\text{asym}} = 0.015$  and  $F_y^{\text{max}} = 0.28$  MN). The asymmetric short-circuit of tiles through the plasma (responsible of important sideways forces

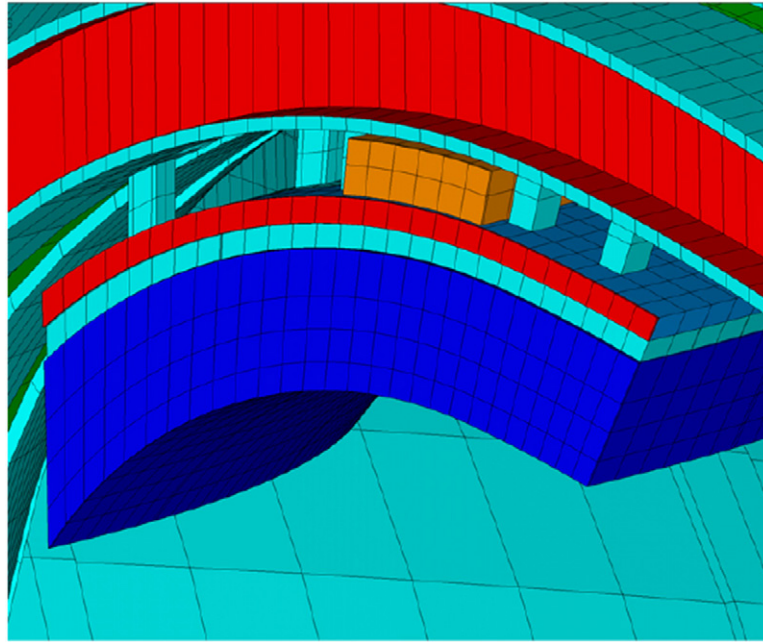


**Figure 12.** Modified model to assess the effect of divertor structures on sideways force: dump plates are toroidally continuous with an equivalent thickness of about 10 cm; the orange elements (insulated from the rest of the structure) represent the divertor coils.

in upward AVDEs) has, instead, limited impact on the global toroidal resistance of the divertor which mainly depends on the resistance of the thick support structure. For this reason the induced current remains, in downward VDEs, essentially symmetric regardless of the toroidally asymmetric contact between plasma and divertor.

Furthermore, while the top dump plates and plasma column have similar curvature and can be homogeneously wetted during upward VDEs, in downward cases the plasma is limited by the divertor targets with shorter poloidal length and opposite curvature. Figure 13 shows the maximum poloidal length of CFC tiles that can be wetted (and effectively short-circuited) in the upper (continuous green line) and lower (continuous purple line) vessel region. It appears evident that during upward AVDEs the area short-circuited through the plasma is much wider (and thus the measured asymmetries more important) than during downward cases.

### 5. Phase shift between halo and plasma current asymmetries

The relationship between plasma current and halo current measured asymmetries has also been investigated. In JET, the asymmetry of the halo current is usually measured with a set of 4 toroidal field pick-up (TFPK) coils positioned (in the octants 1, 3, 5 and 7) between the top dump plate and the upper inner wall protection as shown in figure [2]. This location falls, in most of the cases, completely inside the HC loop allowing an estimate of  $I_h$  to be made from the toroidal field measurements:

$$I_h = \frac{2\pi X}{\mu_0} (B_t^{\text{PK}} - B_t^{\text{ext}}); \quad (4)$$

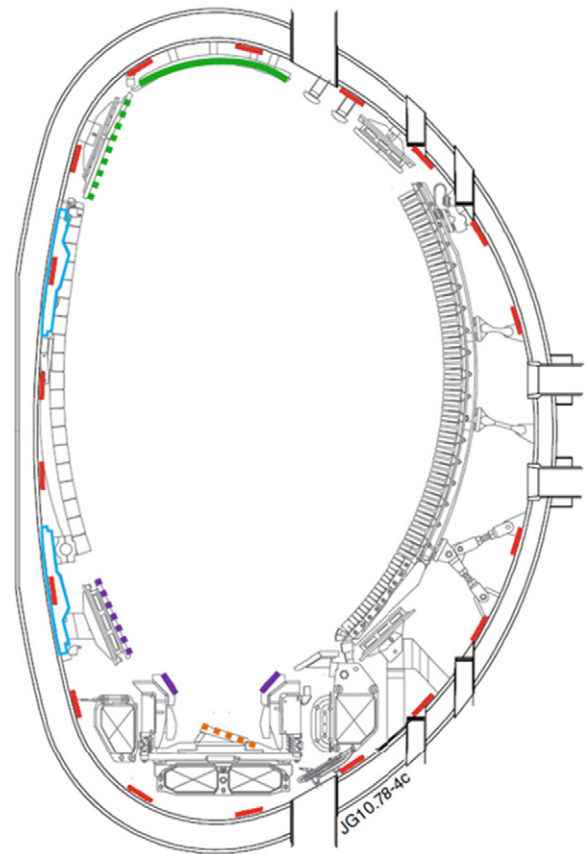


**Figure 13.** Plasma-PFC contact surfaces during VDEs: continuous purple and green lines correspond to area where plasma can effectively short-circuit the divertor and top DP tiles; dashed green and purple lines (inboard wall protections) correspond to area where structures can be wetted but the gaps in toroidal direction are too wide to allow effective short-circuiting through the plasma; contact on top of the LB-SRP (dashed orange) is highly unlikely.

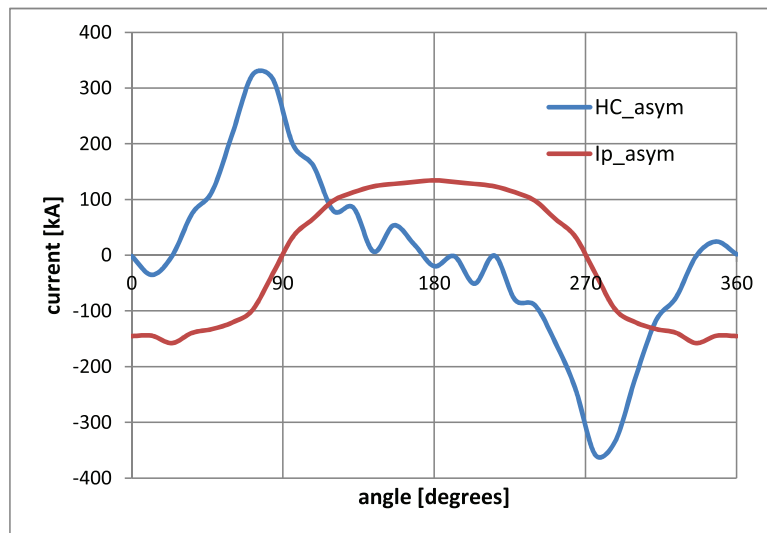


**Figure 14.** Phase shift between plasma current and halo current measured asymmetries (extracted from the FE analysis of locked AVDE with plasma temperature of 15 eV).

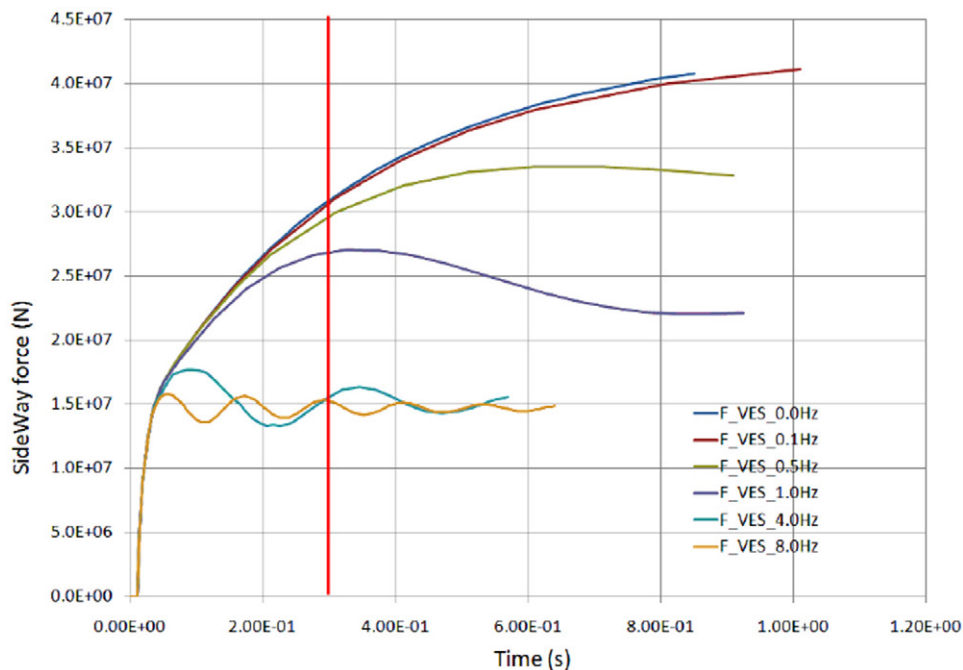


**Figure 15.** Modulus of the horizontal force on ITER tokamak for different AVDE rotation frequencies using the source and sink model.

where  $X$  is the radial location of the pick-up coil,  $B_t^{\text{PK}}$  is the toroidal field measured by the pick-up coil and  $B_t^{\text{ext}}$  is the toroidal field produced by the toroidal field coils.

In case of an  $I_p$  asymmetry, this measure is modified by the toroidal field produced at the pick-up coil location by the ATEC flowing in the bosses connecting the vessel to the top dump plates. Figure 14 shows the halo current as it is measured (at the TFPK coil location and estimated using the formula above) in the FE analysis where no real halo current exists. It can be noticed that the apparent HC asymmetry associated with the ATEC is of the same order of magnitude of the total expected HC. In the specific case of figure 14 the apparent  $I_h$  asymmetry alone would imply a minimum halo fraction of 0.25 (considering

the total  $I_h$  asymmetry = 685 kA; plasma current before disruption = 2700 kA; halo fraction =  $685/2700 = 0.25$ ).

The phase shift between the  $I_p$  and  $I_h$  asymmetry peaks is very close to  $90^\circ$  and is consistent with the JET measurements presented in [8]. The phase shift depends on the toroidal distribution of the ATEC; figure 6 shows that the current flowing from the VV to the dump plates through the bosses is concentrated around  $90^\circ$  and thus, around this location, the TFPK coils measure the highest apparent HC. Nevertheless, depending on the distribution of wetted area in the toroidal direction, the peak of the exchange current between the VV and the dump plates could move toward  $0$  or  $180^\circ$  giving a certain spread to the  $I_p$  versus  $I_h$  phase shift (as reported in [8]).

Since all upward AVDEs are affected by the same bias, reliable information about the HC asymmetries and TPF could be only found in the database of symmetric upward VDEs.

## 6. Comparison with previous analyses

At equal  $A_p^{\text{asym}}$  (0.1), a locked AVDE simulated with the model of asymmetric toroidal eddy current (ATEC) produced the same sideways force as the *source and sink* model [1] generally used for the assessment of AVDE horizontal forces (2.5 MN against 2.6 MN calculated with the source and sink model in a previous FE analysis of JET by the same authors). On the other hand, the maximum horizontal force obtained with the two models during a rotating AVDE appears to be quite different. The source and sink model used to assess loads on ITER vacuum vessel showed that for rotation frequencies higher than 4–8 Hz no additional damping of horizontal force is to be expected and at these frequencies the maximum sideways force is about 50% of the corresponding locked value after 300 ms (red line in figure 15). Applying the ATEC model, the damping of the sideways force appears to be more directly related to the rotation frequency and (as shown in figure 9) at about 170 Hz, the modulus of the sideways force is 10% of the locked one after 30 ms (not yet saturated). To simulate an AVDE through the source and sink model, the current entering and exiting from the structure is imposed in location and intensity while with the ATEC model the current is induced in the structure and due to the finite time constants of involved conductors could depend more strongly on the rotation frequency. The relationship between the sideways force and the rotation frequency needs more investigation as the rotating horizontal force is one of the critical outstanding issues for the ITER tokamak.

In previous work, loads during AVDEs have been supposed to be the effect of direct current exchange ('source' current) between plasma and structures. More likely, as shown in the present analysis and confirmed by the measurements, AVDE loads are caused by asymmetric conductive paths which arise, along the vessel when the kinked plasma asymmetrically wets the wall. Contrary to what was previously supposed, the total current in the structures is the same at all toroidal positions. As a consequence, all loads caused by the interaction of the 'source' current flowing in toroidal direction with the poloidal field would be reduced significantly.

## 7. Conclusions

All the main asymmetry related parameters measured at JET during locked and rotating AVDEs are reasonably well reproduced assuming the sideways force caused by an asymmetric distribution of toroidal eddy currents in the conductive structure. Independent of the physics mechanism responsible for the asymmetrical short circuits of the PFCs through the plasma, the simulations and the measurements (in particular the phase relationship between  $\Delta I_p$  and  $\Delta M_{Tz}$ ) show that an asymmetric current of the same sign as the

plasma current flowing at a location near to the top dump plates is very likely. Furthermore, if this asymmetric current has the same value of the measured  $\Delta I_p$ , the resulting sideways force is close to the values calculated with other methods (source and sink) and inferred from mechanical measurements.

It has also been shown that the ATEC model applied to downward AVDEs produces negligible sideways forces confirming what experienced at JET. It appears that sideways forces can be prevented if, during AVDEs, the plasma is limited by a conductive, toroidally continuous structure with low resistance compared to the vessel (like the divertor support). ATEC are also responsible for a significant part of the measured asymmetry of HC (and thus for part of the measured TFP) as they affect the toroidal field at the location where HC measurements are taken. In fact, for upward VDEs  $I_p^{\text{asym}}$  and HC asymmetry could just be different measurements of the same current. On the other hand HC asymmetries and TPF measured during downward VDEs should be free from this bias and would allow reliable estimate of HC asymmetries and TPF. Unfortunately because of lack of reliable diagnostic in the divertor region there are few available measurements of HC in opposite octants during downward VDEs. Nevertheless from these limited data [8] appears that also HC asymmetries during downward VDEs ceased after the installation of the divertor.

The model and the analyses presented in this work do not attempt to explain the reasons of plasma asymmetries and rotation during disruptions, still they explain the reasons of the loads that originate from those asymmetries and reproduce well all phenomena observed in the experiments.

## Acknowledgment

This work has been carried out within the framework of the EUROfusion Consortium and has received funding from the Euratom research and training programme 2014–2018 under grant agreement No 633053. The views and opinions expressed herein do not necessarily reflect those of the European Commission or of ITER IO.

## References

- [1] Riccardo V. et al 2000 *Nucl. Fusion* **40** 1805
- [2] Pautasso G. et al 2011 *Nucl. Fusion* **51** 103009
- [3] Evans T. 1997 *J. Nucl. Mater.* **S241–3** 606
- [4] Bachmann C. Asymmetric loads on the ITER tokamak components due to the sink and source model, ITER\_D\_356AD2 v1.1 private communication
- [5] Riccardo V. 1997 *EU Physics Task Report: Physics Guideline for Sideway Force on Vacuum Vessel during VDEs* 12/2007
- [6] Wesson J. *Tokamaks* (Oxford science publications)
- [7] Gerasimov S.N. et al 2014 Plasma current asymmetries during disruptions in JET *Nucl. Fusion* **54** 073009
- [8] Riccardo V. et al 2009 Progress in understanding halo current at JET *Nucl. Fusion* **49** 055012
- [9] Romanelli F. et al 2015 *Nucl. Fusion* **55** 104001